ACS OMEGA

Open Access

http://pubs.acs.org/journal/acsodf

Article

Characteristics, Source Apportionment, and Health Risk of Heavy Metals in the Soils of Peri-urban Shanghai Chongming Island

Cheng Shen, Min Wang, Jinghua Su, Huilun Sun, Wenan Hu, Kuangfei Lin, Jian Wu, Fuwen Liu, Xiurong Chen,* and Chenyan Sha

Cite This: *ACS Omega* 2024, 9, 42734−42745

Read Online

ACCESS | Metrics & More | Article Recommendations | Supporting Information

ABSTRACT: Heavy metals resulting from human activities pose significant threats to human health and the soil ecosystem. In the current study, 917 soil samples from Chongming Island in Shanghai, China, were examined for eight heavy metals. The sources of contamination were identified by using a Positive Matrix Factorization (PMF) model. Meanwhile, spatial interpolation and Moran's *I* index were applied to validate the model in terms of spatial linkages. The results revealed that the average concentrations of As, Cd, Hg, Pb, Cr, Cu, Zn, and Ni in the soil were 8.87, 0.19, 0.06, 28.75, 76.01, 37.74, 88.93, and 30.33 mg kg^{-1}, respectively. The PMF analysis proved that heavy metals in the soil of the study area are mainly influenced by traffic sources (Cr and Pb), industrial sources (Zn, Cd, and Cu), station sources (Hg), and natural sources (As and Ni), with contribution rates of 22.23, 26.25, 36.38, and 15.14%, respectively. The combination of Moran's index and the spatial analysis method not only verified the analytical results of the receptor model on the one hand but also served as a supplementary explanation for the sources of heavy metals in the soil. The health risk assessment indicated that noncarcinogenic values were below the threshold values. The total carcinogenic risk (R_T) of different heavy metals has a descending order of Cr > As > Ni > Cd. The R_T values of multiple heavy metals for children and adults were 5.28×10^{-04} and 4.10×10^{-05}, respectively, which were close to the risk threshold. Therefore, attention should be paid to the health risks, especially for children's skin contact, which is the main exposure pathway.

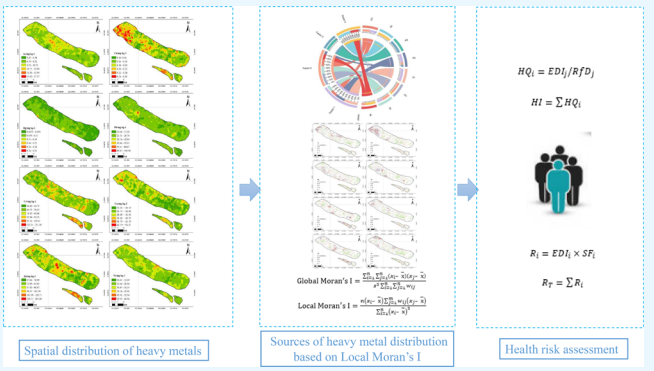

1. INTRODUCTION

As one of the most important ecosystems for maintaining the balance of energy flow and material circulation, soil is the main medium involved in material transfer and transformation in nature.[1,2] In recent years, the prevention and control of soil pollution have gradually become the focus of social attention. In March 2022, the Ministry of Ecology and Environment of China issued a document proposing specific requirements for strengthening the control of heavy metal pollutant emissions and effectively preventing and controlling environmental risks related to heavy metals. Compared with other pollutants, soil heavy metal pollutants accumulate easily and closely related to their parent materials and human activities, which have spatial heterogeneities.[3−6] They also present a constant threat to both the natural ecosystem and human beings.[7,8] Heavy metal pollution has become a worldwide environmental problem.[9−11] Soil pollution by heavy metals has accelerated in China in the last two decades owing to the rapid economic development and industrialization.[12] Once heavy mental pollutants exceed the self-purification capacity of the soil, they pose a threat to soil productivity and production potential and to human health through food chain transmission.[13−15] These elements are derived from both anthropogenic sources, such as emissions and agricultural activities, as well as natural processes, including precipitation, atmospheric sedimentation, and weathering.[16,17] Therefore, clarifying the characteristics, source distribution, ecological effects, and health risks of soil heavy metal pollution is an important prerequisite for soil pollution prevention and control.[18]

Heavy metals in soil have characteristics such as concealment, hysteresis, accumulation, and irreversibility, which pose serious hazards. Heavy metals in soil can be absorbed by plant roots, migrate and transform through soil root system plant aboveground parts, and have a significant impact on human health through food chain transmission.[19,20] Excessive intake of heavy metals into the human body can cause damage to the kidneys, liver, and bones and even lead to serious systemic

Received: April 16, 2024
Revised: September 12, 2024
Accepted: September 23, 2024
Published: October 8, 2024

health problems. Therefore, fully exploring the health risks of soil heavy metals under different sources can help achieve refined environmental management of soil heavy metal pollution and protect the ecological environment and human health.

As the largest alluvial estuarine island in China, Chongming Island is in the Yangtze River Estuary, and half of its present area was obtained through reclamation of wetlands. Accounting for nearly one-half of Shanghai's land area, the soil environmental quality of Chongming is significant in ensuring regional agricultural products, the safety of the drinking water, and other ecological services. With the increasing attention paid to soil quality and management, a series of studies have been conducted on the heavy metal distribution in soils.[21−24] Identifying the sources of heavy metal pollutants in soil especially from anthropogenic source is an important step in the implementation of source control, which is of great significance to the prevention and control of soil heavy metal pollution, economic development, and human health.[25,26]

At present, methods of source apportionment involve source identification and quantification.[27,28] The receptor model is a source analysis technique that qualitatively identifies the types of sources of the pollutants in soil samples and quantitatively determines the contributions of each pollution source.[29] The existing receptor models mainly include the known source component spectral method (Chemical Mass Balance, CMB)[30,31] and the unknown source component spectral method (Positive Matrix Factorization, PMF),[32,33] principal component multiple linear regression (Absolute Principal Component Score-Multiple Linear Regression, APCS-MLR),[34,35] and the UMIX model.[36−38] Among those, PMF advocated by the U.S. Environmental Protection Agency (EPA) emerges as an ideal model for both identifying and quantifying pollution sources. PMF adeptly dissects the initial database into a contribution matrix and discrete profile group, facilitating precise determination of contribution and source delineation (U.S. EPA, 2014).[39,40] However, owing to the complexity of the spatial variability of soil heavy metal contents and their diversity, it is difficult to meet the requirements for the quantitative contribution to the pollution analysis using a single scale as the source of the analytical method. It is still impossible to accurately identify the specific sources of pollutants when the source component spectrum is unknown. Spatial autocorrelation refers to the scenario in which some of the variables in the same or different distribution areas are potentially interdependent of the observation data.[41,42] The bivariate Moran's *I* compared two factors in space through index calculation to characterize the spatial correlation between the two factors. Liu et al.[43] used the double variable local Moran's index of the city, county, and Hunan Province to identify soil heavy metal sources and the spatial relationships with enterprises, rivers, and roads. Han and Xu[44] used geostatistics and spatial autocorrelation to quantitatively analyze the soil sources in Zhangqiu City, Shandong Province, and verified the validity of their spatial autocorrelation analysis as well. Combining the PMF model with Moran's *I*, the applications would function as a potent tool for effectively identifying contamination.[45] However, there are few studies that have investigated the amalgamation and comparison of different approaches in the vicinity of a megacity.

Based on the above discussion, the main purpose of our research is to (a) use geostatistical methods to study the spatial distribution of Cd, Pb, As, Cr, Cu, Ni, and Zn in soil; (b) complete the determination of the sources of the soil heavy metal distribution by PMF and Moran's *I*; and (c) determine the potential health risks of heavy metals via three routes of ingestion, inhalation, and dermal exposure.

2. MATERIALS AND METHODS

2.1. Study Area. The Chongming District (31.45−31.85° N and 121.16−121.90° E) in the Yangtze River Estuary in China is the largest alluvial estuarine island in China, consisting of Chongming Island, Changxing Island, and Hengsha Island. Among them, Chongming Island is the third largest island in China, and it has a northern subtropical ocean climate, with an average annual temperature and precipitation of 15.3 °C and 1117.1 mm.

2.2. Sampling and Analytical Procedures. A total of 917 (the number was the sum of the original sampling point deducted by nonagricultural land) soil samples were collected based on the area and distribution of agricultural land in Chongming area from March to June in 2020, combined with the grid method and 3S technology, using a 1 × 1 km grid for agricultural land distribution in the three islands of the entire area. The distribution of the sampling sites is shown in Figure. 1. During the sampling, soil samples were collected according

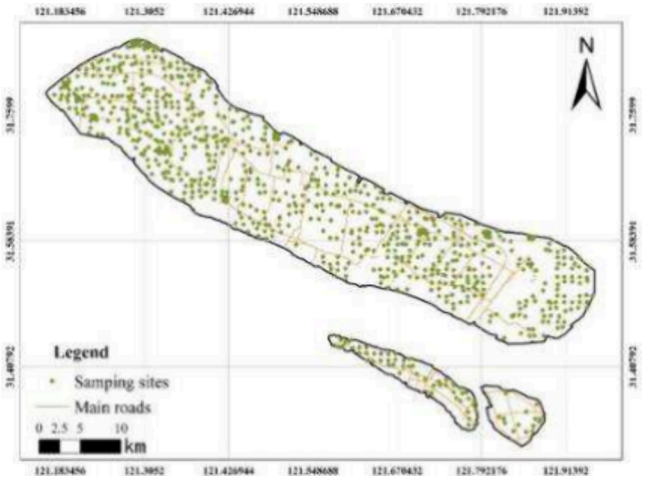

Figure 1. Distribution of sampling sites.

to the Technical Specifications for Soil Environmental Monitoring (HJ166-2004) using stainless steel shovels within a 1 × 1 km sampling grid. Each sample was a mixture of five soil cores: one was collected in from the center, and four were from the corners of the double-diagonal pattern. Each sample consisted of 2 kg of fresh soil. In the laboratory, the soil samples were air-dried with little light, and the debris from animals, plants, and the gravel were removed. The soil samples were ground, passed through a 100-mesh polyethylene sieve, and then stored in a paper bag prior to analysis.

All the soil samples were digested in a polytetrafluoroethylene system using a mixture of HF (1 mL), HNO_3 (5 mL), and $HClO_4$ (1 mL) at 180 °C for 10 h. The concentrations of Cd, Pb, As, Cr, Cu, Ni, and Zn in the digester were determined via inductively coupled plasma-mass spectrometry (ICP-MS, Agilent 7500a, USA). The detection limits for Cd, Pb, As, Cr, Cu, Ni, and Zn were 0.01, 2.50, 0.01, 0.25, 0.10, 0.10, and 0.50 $mg \cdot kg^{-1}$, respectively. After the soil samples were digested using 5 mL of aqua regia and 5 mL of deionized water at 100 °C for 4 h, the concentration of Hg was determined using an

https://doi.org/10.1021/acsomega.4c03647
ACS Omega 2024, 9, 42734−42745

atomic fluorescence mercury meter (AFS, AFS-9330 Jitian Analytical Instrument Co., Beijing, China), and the laboratory detection limit for Hg was 0.001 mg·kg^{-1}. During the sample analysis and testing, a standard reference material (GSS-1, the National Research Center for Certified Reference Materials of China) was used for quality control. The recovery of each element was controlled at 100 ± 10%, and the relative standard deviation between parallel samples was less than 20%.

2.3. Source PMF Model. In this study, the PMF5.0 model developed by the United States Environmental Protection Agency (U.S. EPA) was used to analyze the sources of the heavy metals in the agricultural land in Chongming District. Positive definite PMF, a multivariate factor analysis method proposed by Paatero et al.,[32] has been widely used in the analysis of the sources of environmental pollutants. In this model, the original matrix X is decomposed into a source contribution matrix g, a source component spectrum matrix f, and a residual matrix e.[46] The calculation formula is as follows:

$$x_{ij} = \sum_{k=1}^{p} g_{ik} \times f_{ik} + e_{ij} \tag{1}$$

where x_{ij} is the content of element j in the ith soil sample; g_{ik} is the contribution of the kth source to the ith sample; f_{tk} is the content of the ith element in the kth source; e_{ij} is the residual matrix; and e_{ij} is calculated by defining the target function.

The objective function q is defined as follows:

$$q = \sum_{i=1}^{n} \sum_{j=1}^{n} \left(\frac{e_{ij}}{uij} \right) \tag{2}$$

where x_{ij} is the uncertainty of element j in the ith soil sample. Each individual data point can be weighted and given an appropriate uncertainty size. The uncertainty is calculated using eqs 3 and 4. When the concentration of each element is less than or equal to the corresponding method detection limit (MDL), the uncertainty is

$$u = \left(\frac{5}{6} \right) \times \mathrm{MDL} \tag{3}$$

When the concentration of each element is greater than the corresponding MDL, the uncertainty is

$$u = \sqrt{(\delta \times C)^2 + 0.5\mathrm{MDL}^2} \tag{4}$$

where δ refers to the relative deviation, C is the element's concentration, and MDL stands for the method detection limit.

2.4. Spatial Autocorrelation Analysis (Calculations). Spatial autocorrelation, which can be used to estimate the value of one variable in different spatial positions, was adapted to analyze the characteristics and spatial distributions of the heavy metal accumulation in the agricultural land in Chongming District. In addition, it is often used to measure the aggregation degree of variables in a spatial domain and analyze the characteristics of the spatial−temporal evolution. The spatial autocorrelation indexes can be divided into the Global Moran's I and the Anselin Local Moran's I.[47]

1) The Global Moran's I is an effective method for identifying the aggregation or dispersion of attribute values in the entire region.

$$\text{Global Moran's } I = \frac{\sum_{i=1}^{n} \sum_{j=1}^{n} (x_i - \overline{x})(x_j - \overline{x})}{s^2 \sum_{i=1}^{n} \sum_{j=1}^{n} w_{ij}} \tag{5}$$

$$s^2 = \frac{1}{n} \sum_{i=1}^{n} (x_i - \overline{x})^2 \tag{6}$$

Moran's I ranges from $[-1, 1]$. $I > 0$ indicates a positive spatial correlation, $I < 0$ indicates a negative spatial correlation, and $I = 0$ indicates that the spatial elements tend to be random in the entire region. n is the number of units in space, x_i and x_j are the attribute values of spatial elements i and j, and w_{ij} is the space weight coefficient matrix and represents the proximity of each spatial element.

2) The Local Moran's I was adapted. The location of a spatial agglomeration or an isolated area of spatial element attribute values and the locations of outliers were studied. This index measures the various clustering values and regions. The spatial distribution of each spatial unit in the study area was analyzed. According to the value of each unit, the spatial pattern was analyzed, and the equation used to calculate the Local Moran's I is as follows:

$$\text{Global Moran's } I = \frac{n(x_i - \overline{x}) \sum_{j=1}^{m} w_{ij}(x_j - \overline{x})}{\sum_{i=1}^{n} (x_i - \overline{x})^2} \tag{7}$$

$I_i > 0$ indicates a significant positive spatial autocorrelation between the regional spatial unit i and the adjacent spatial unit j, and $I_i < 0$ indicates a significant negative space autocorrelation. n is the number of units in the space, x_i and x_j are the attribute values of spatial elements i and j, and w_{ij} is the spatial weight coefficient matrix.

2.5. Exposure Assessment Calculation. Health risk assessment is a method to assess carcinogenic and non-carcinogenic health risks by calculating the absorption amount of human exposure to chemicals. The exposure routes of residents' heavy metals mainly include hand and mouth intake, respiratory inhalation, and skin contact. The health risk assessment method recommended by the U.S. EPA was used to identify the degree of risk to human health from heavy metal elements.[48,49] The formulas for calculating the intake dose under different exposure paths are as follows:

$$\mathrm{EDI_{ing}} = \frac{C \times \mathrm{IR_{Soil}} \times \mathrm{EF} \times \mathrm{ED}}{\mathrm{BW} \times \mathrm{AT}} \times 10^{-6} \tag{8}$$

$$\mathrm{EDI_{dermal}} = \frac{C \times \mathrm{SA} \times \mathrm{AF} \times \mathrm{ABS} \times \mathrm{EF} \times \mathrm{ED}}{\mathrm{BW} \times \mathrm{AT}} \times 10^{-6} \tag{9}$$

$$\mathrm{EDI_{inh}} = \frac{C \times \mathrm{IR_{Air}} \times \mathrm{EF} \times \mathrm{ED}}{\mathrm{PEF} \times \mathrm{BW} \times \mathrm{AT}} \times 10^{-6} \tag{10}$$

EDI_{ing}, EDI_{dermal}, and EDI_{inh} (mg/kg·day) represent the average daily intake from ingestion, dermal, and inhalation absorption, respectively. C is the measured value of the heavy metal content in the sample. The meanings and values of other parameters are shown in Table S1.

2.6. Noncarcinogenic and Carcinogenic Risk Assessment. Different routes of entry of heavy metals into the body (ingestion, dermal contact, and inhalation) were considered, and the health risks from heavy metal contamination for

https://doi.org/10.1021/acsomega.4c03647
ACS Omega 2024, 9, 42734−42745

Table 1. Distribution Characteristics of the Soil Heavy Metal Contents (n = 917)

	min (mg·kg^{-1})	max (mg·kg^{-1})	mean (mg·kg^{-1})	median (mg·kg^{-1})	local background (mg·kg^{-1})	SD	coefficient of variation (%)
As	4.09	17.27	8.87	8.11	9.10	1.64	0.18
Cd	0.10	0.38	0.19	0.18	0.13	0.07	0.38
Hg	0.004	0.31	0.06	0.06	0.10	0.03	0.48
Pb	13.60	144.00	28.75	23.20	25.47	7.45	0.26
Cr	46.00	211.00	76.01	74.00	75.00	18.06	0.24
Cu	12.00	116.00	37.74	27.00	28.59	9.45	0.25
Zn	47.00	201.00	88.93	80.00	86.10	18.59	0.21
Ni	14.00	61.00	30.33	29.00	31.90	4.90	0.16

different populations (adults and children) were assessed. The potential ecological risk is expressed by the following Equations:[50]

$$HQ_i = EDI_j/RfD_j \quad (11)$$

$$HI = \sum HQ_i \quad (12)$$

HQ_i and HI are, respectively, the noncarcinogenic risks caused by heavy metal i and the sum of noncarcinogenic risks caused by multiple exposure routes j; RfD_j represents the toxicity reference dose of elements under different exposure routes; and EDI_j is the pollution dose of soil ingested by hand and mouth, skin, and respiratory inhalation. Based on the actual situation of the study area and specific reference to relevant scholars, the reference values are displayed in Table S2. HI or $HQ_i \leq 1$ means that there is no obvious harm to human beings, a value > 1 is very likely to be harmful, and a value ≤ 10 means that there is a serious chronic risk.

$$R_i = EDI_i \times SF_i \quad (13)$$

$$R_T = \sum R_i \quad (14)$$

R_i refers to the carcinogenic risk caused by the heavy metal pollution dose ingested under the three exposure routes of hand and mouth, skin, and respiration; R_T is the sum of carcinogenic risks caused by different soil heavy metals in each route; and SF_i is the slope coefficient of carcinogenic risk of the three exposure routes of hand and mouth, skin, and respiration, with the unit of mg·(kg·d) $^{-1}$.

2.7. Data Processing and Analysis. Excel 2013 and SPSS 20.0 were used for the preprocessing statistical analysis of the heavy metal values, and the EPA's PMF 5.0 software was used for the heavy metal source analysis;

Origin 9.1 and ArcGIS 10.8 were used for the mapping and spatial interpolation, and Geoda 1.18 was used for the spatial correlation analysis based on Moran's I.

3. RESULTS AND DISCUSSION

3.1. Descriptive Statistics of Heavy Metals in Soil. The descriptive statistics of the heavy metals are summarized in Table 1. The average concentrations of As, Cd, Hg, Pb, Cr, Cu, Zn, and Ni in the soil were 8.87, 0.19, 0.06, 28.75, 76.01, 37.74, 88.93, and 30.33 mg kg^{-1}, respectively. The maximum values of Pb and Cu were 5.65 and 4.06 times greater than their background values, respectively. The percentages of the area in Shanghai where the background values were exceeded were 43% for Cd, 13% for Pb, 1% for Cr, 32% for Cu, and 3% for Zn. The coefficient of variation (CV) not only reflects the degree of variation and the uniformity of the contents of certain metals among the sampling sites but also reflects the effects of human activities on the heavy metal pollution.[51] The coefficients of variation are as follows: Hg (0.48) > Cd (0.38) > Pb (0.26) > Cu (0.25) > Cr (0.24) > Zn (0.21) > As (0.18) > Ni (0.16). In the current study area, the notable standard deviation and coefficient of variation for Hg (0.48) and Cd (0.38) indicated substantial spatial variability, suggesting elevated levels at specific locations potentially influenced by external factors, such as long-term agricultural practices and industrial activities.[52] Furthermore, the mean values of Pb, Cu, and Zn were notably higher than their respective medians, indicating abnormal distributions of the concentration with positive skewness and cliffy kurtosis. These results provide further evidence of the external inputs of heavy metals in soils. And the soil in a localized area was obvious and accompanied by regional construction and development. The heavy metals in agricultural soils in the Chongming District have been affected by human activities to some extent.

3.2. Spatial Distribution of Heavy Metals in Soil. The spatial distribution characteristics of the soil heavy metals that were determined using the Ordinary Kriging (OK) interpolation method are shown in Figure 2. The root-mean-square standardized error values indicate that the accuracy of the interpolation is acceptable. The spatial distribution patterns of Cd and Cu were similar. The hotspots were concentrated in the northwestern and central regions of the study area, whereas the values were lower in the eastern region, which exhibited a decreasing trend from the northwest to southeast. The concentrations of Cr and Zn were higher in the middle of Chongming Island and Changxing Island but lower in the northwestern and southeastern parts of the study area, which suggested a decreasing trend from the middle to both sides. The concentrations of Pb were higher in the central and western regions of the study area and lower in the rest of the study area, which exhibited the characteristic of high local accumulation, and anthropic inputs generally caused significant enrichment of Pb in the soils. Except for the high values in the middle of the region, the As and Ni contents were low, which indicated that the anthropic contributions of As and Ni were low. This spatial distribution pattern directly reflects the possible sources of the soil heavy metal accumulation and provides a foundation for subsequent source model analysis.

3.3. Sources of Heavy Metals. The PMF model employs a weighted least-squares fit with uncertainty and error propagation problems appropriate for source profiles.[16] This model was utilized to quantify the contributions from various sources of heavy metals and confirm the sources of the heavy metals in agricultural soils. The standard deviations of measured concentrations for each element at specific points were selected as uncertainty data. Factor numbers (3−6) were set for multiple iterative calculations. As the number of factors was confirmed to be 4, Q (Robust)/Q (True) declined rapidly. The residual was between −3 and 3. The fingerprint was

https://doi.org/10.1021/acsomega.4c03647
ACS Omega 2024, 9, 42734−42745

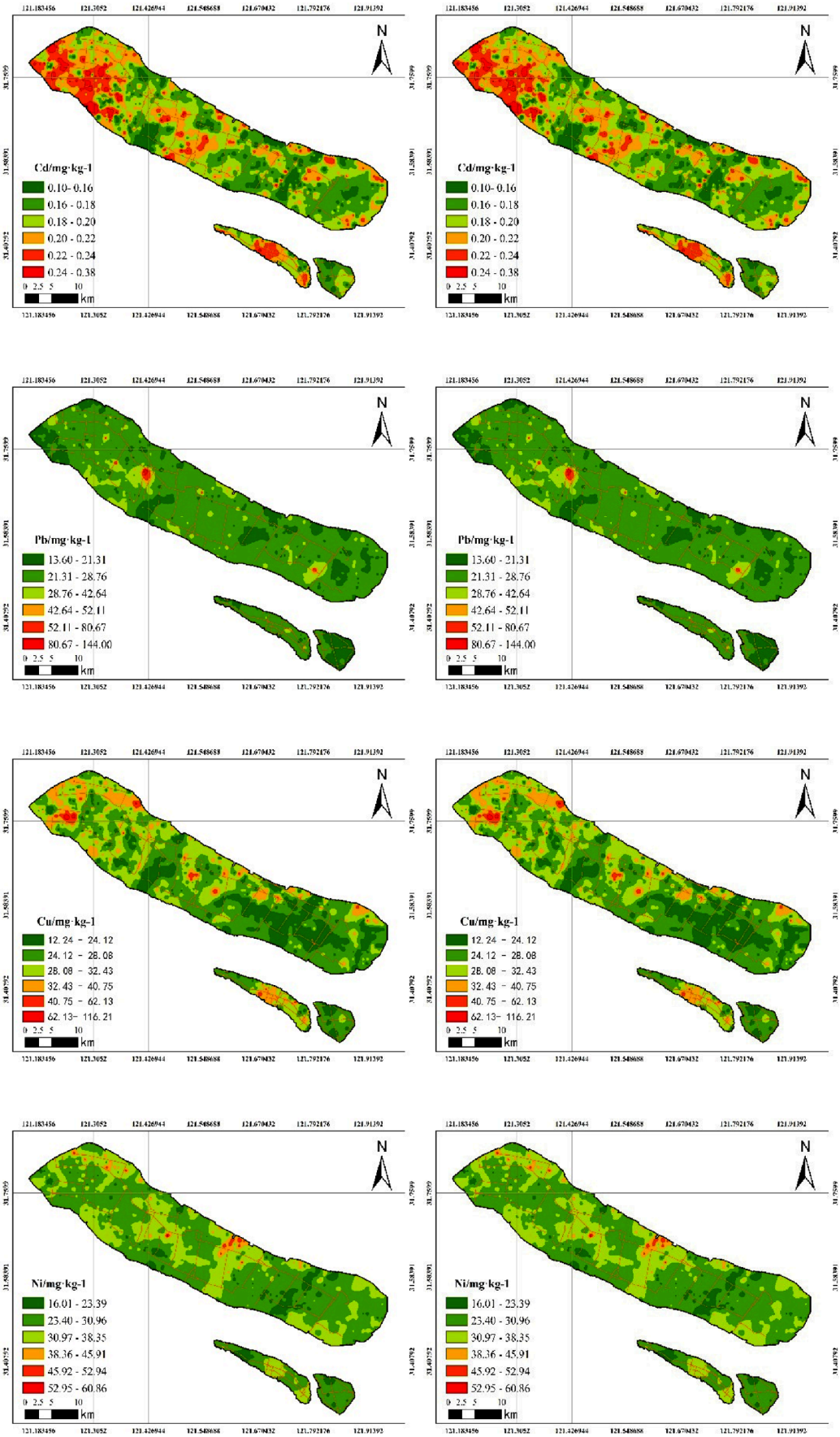

Figure 2. Spatial distributions of soil heavy metals.

https://doi.org/10.1021/acsomega.4c03647
ACS Omega 2024, 9, 42734−42745

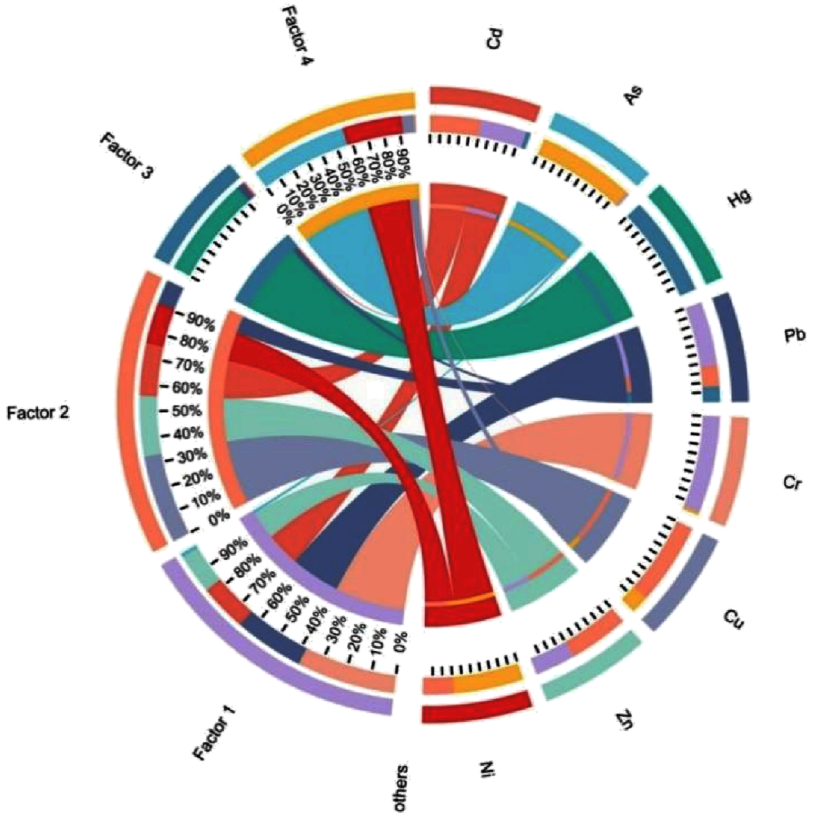

Figure 3. Contributions of different factors to the heavy metals in the soil obtained using the PMF model.

obtained after rotation at Fpeak = 0.5. The contribution rates of the four factors to the heavy metals are displayed in Figure 3. The rotated component matrix shows that Cr and Pb were associated with the first component (F1). The second component (F2) included Cu, Zn, and Cd, and the third component (F3) contained Hg. As and Ni were in the fourth component (F4).

Cr and Pb had a relatively consistent source, which was predominately controlled by F1, with a percentage of 97.9 and 68.8%, respectively. Cr and Pb in the soil of the study area are moderately variable, and the average values are higher than the background values of soil elements in Shanghai, which mean that the soil Cr and Pb in the study area have been affected by human activities. Relevant studies have shown that Pb is a symbolic element of vehicle exhaust emissions in traffic activities.[53] The exhaust emissions of vehicles using leaded gasoline cause PB to enter the surrounding environment. Although leaded gasoline has been banned in Chongming District, the standard for lead-free gasoline mainly requires a lead content of less than 0.013 $g \cdot L^{-1}$. Small amounts of lead-containing compounds and particles still exist in automobile exhaust. It was discovered that the high values of Cr and Pb were distributed at the intensive intersections of the traffic network. The high values were in the central and western regions of the Chongming District, containing two local parks with heavy traffic. The high-value area in the southeast is the junction of two highways and is also the only entrance to and exit from Chongming Island. Over the past 50 years, it was identified that vehicle emissions were the main source of lead in agricultural soils.[54,55] Xie et al.[56] also found that Pb in agricultural soils was closely related to transportation in Baoshan District (Shanghai). Therefore, it is speculated that F1 is the traffic source.

F2 explained 87.7, 60.4, and 51.7% of Cu, Zn, and Cd, respectively. According to the spatial distributions of Cu, Zn, and Cd, the contents of Cu, Zn, and Cd were higher in the northwestern and central regions of the study area. Through field investigation, it was found that many heavy-metal-related enterprises, such as metal structure manufacturing, metal surface treatment and heat treatment, and steel rolling processes, were located near the high-value area. Negahban and Mokarram[57] reported that the source of Cu and Zn may be affected by an aluminum plant and the surrounding industrial activities. It was also found that the Cu contents of the different types of soil were influenced by pesticides, and Cu is a degerming agent. In addition, nonagricultural factors, such as industrialization, also made significant contributions. In heavy metal enterprises, compound production, byproducts, and alloy production processes are often accompanied by Cd, Cu, and Zn complexes. Through atmospheric precipitation and surface runoff into the soil, the heavy metals in industrial waste led to enrichment of these heavy metals. Therefore, F2 is inferred to be an industrial source dominated by heavy metal processes.

Hg was dominantly controlled by F3, with a percentage of 100%. And the coefficient of variation (0.48) was the highest among the eight metals, which suggested that the metals may be contaminated by point sources. Based on the spatial distribution shown in Figure 2, it was determined that the high Hg contents were distributed in the southwest coast and coincided with the location of the Chongming wharf and coach station. It has been determined that exhaust gas from ships fueled by oil and natural gas cause atmospheric Hg pollution.[58]

https://doi.org/10.1021/acsomega.4c03647
ACS Omega 2024, 9, 42734−42745

Table 2. Global Moran's *I* and Related Parameters

index	As	Cd	Cr	Cu	Ni	Pb	Zn	Hg
Global Moran's *I*	0.01	0.35	0.91	0.08	0.15	0.06	0.14	0.28
Z score	0.07	1.66	4.79	0.39	0.22	0.31	0.65	1.35
P value	0.94	0.10	0.11	0.69	0.47	0.75	0.52	0.18

Then, Hg could indirectly pollute the soil through dry and wet deposition. Therefore, it can be speculated that F3 was related to the exhaust gas from ferries, automobiles, and the surrounding refueling facilities.

As and Ni were predominately controlled by F4 with percentages of 96.3 and 59.3%, respectively. According to the descriptive statistical analysis, the average values of As and Ni were lower than the background values of soil pollution in Shanghai. In addition, the degree of variation was low, which indicated that the two elements were less affected by human activities. Figure 2 shows that the spatial distributions of these two heavy metals were similar, with a wide range and low values. Numerous studies have proven that the contents of Ni and As in soil are mainly affected by natural geological background factors and have no significant correlation with human activities.[59−61] Hu et al.[62] also explored the topsoil in parks in an urban area in Lanzhou, and their results revealed that As and Ni contents were significantly correlated with the main products of the soil's parent material, so F4 is concluded as a natural source.

3.4. Spatial Autocorrelation of Soil Heavy Metals. We use the Kolmogorov−Smirnov test to test the normal distribution of the data itself before data analysis. The normal distribution test results of eight heavy metal contents in soil are shown in Table S4. It can be seen that the significance level of all heavy metals is less than 0.05, rejecting the null hypothesis that the population from which the sample comes has no significant difference from the normal distribution. These data do not follow a normal distribution. Therefore, we perform a logarithmic or square root transformation on the raw data before the Moran analysis. The spatial correlation index. Global Moran's *I*, and the related parameters of the eight heavy metals were calculated using ArcGIS 10.8 (Table 2). All eight heavy metals in the agricultural soil from Chongming exhibited positive spatial correlations with Global Moran's *I*, from the highest to the lowest, as follows: Cr (0.91), Cd (0.35), Hg (0.28), Zn (0.14), Cu (0.08), Pb (0.06), Ni (0.15), and As (0.01). All values greater than zero suggest a notable level of spatial autocorrelation. The *Z* score represents the number of standard deviations, and when the large value of the *Z* score is used, it directs an aggregation state in the spatial distribution. Thus, based on the comprehensive analysis of the *Z* score and *P* value, the multiple of the standard deviation and the probability of generating random patterns for Cr and Cd exhibited a strong spatial correlation and obvious clustering characteristics, whereas Ni and As exhibited a random distribution.

To further explore the characteristics of the local spatial distributions of the soil heavy metals, the Local Moran's *I* was adopted, aiming to analyze the clustering characteristics of the observed values within the local scope and the locations of the inferred outliers to obtain the cluster distribution results for the soil heavy metal contents (Figure 4). There were five types of clustering: high value clustering (H−H), low value clustering (L−L), low values surrounded by high values (L−H), high values surrounded by low values (H−L), and no clustering. H−H represents areas with high-value accumulation, L−L denotes areas with low-value accumulation, L−H designates areas with low-value anomalies, H−L signifies regions with high-value anomalies, and no clustering indicates samples lacking statistically significant patterns. The H−H areas for Cr and Pb only occurred on both sides of the main traffic lines and did not coincide with the other point source factors. A considerable number of L−L areas also existed in the eastern region of Chongming, which indicated that there was a certain correlation between the high Cr and Pb contents and the traffic network. Huang et al.[63] used a random forest regression model to illustrate that the traffic was significantly correlated with the Pb and Cr contents. Based on the analysis of the Local Moran's *I* index, source 2 was identified as the traffic source. Cd, Cu, and Zn mostly exhibited H−H points, which were distributed in the western part of Chongming Island. Moreover, these sites were accompanied by numerous L−H sites corresponding to Figure 4. The Cd, Cu, and Zn contents were significantly correlated with the distribution of the enterprises. It was also found that raw materials containing heavy metals, such as Cd, Zn, and Cu, were used in industrial production. The wastes generated by the production processes were discharged into the soil, thus resulting in the accumulation of heavy metals, which further confirmed that source 2 was mainly an industrial source of heavy metals. The clustering results showed that the H−H and L−H Hg sites were distributed in the southern part of Chongming Island along the Yangtze River. Most of the L−L sites were concentrated in the upper area and on both sides of Chongming Island. Based on the high variation coefficient of Hg, point source pollution may be possible. Therefore, it is reasonable to conclude that source 3 was vehicle exhaust, petrol pump vapor from the wharfs, and bus stations. The L−L sites for As and Ni did not correspond to the transportation network or enterprise distribution, which were consistent with the characteristics of a natural source. The contribution rate of source 4 was >50%, and the spatial distributions were also similar, which suggested that As and Ni were affected by the same factors. Therefore, it is reasonable to conclude that source 4 was a natural source.

3.5. Health Risk Assessment of Heavy Metals in Soil. Based on the exposure risk evaluation model and corresponding related parameters, the results of noncarcinogenic and carcinogenic risks under different exposure paths are shown in Tables 3 and 4. The total noncarcinogenic risk (HQ) of the three different exposure routes varies greatly, among which the risk of hand and mouth intake is the highest, followed by skin contact, and the risk of respiratory inhalation is the lowest. These research results are consistent with previous studies.[64,65] The total noncarcinogenic risk (HQ) of different heavy metal elements is ranked as As > Cr > Pb > Hg > Ni > Cu > Zn > Cd in descending order. Although the degree of noncarcinogenic risk of different heavy metal elements in soil varies, they do not reach the upper limit of acceptable noncarcinogenic risk (HQ ≤ 1): the risk is small or negligible, which indicates that a single element does not generate noncarcinogenic risk to the

https://doi.org/10.1021/acsomega.4c03647
ACS Omega 2024, 9, 42734−42745

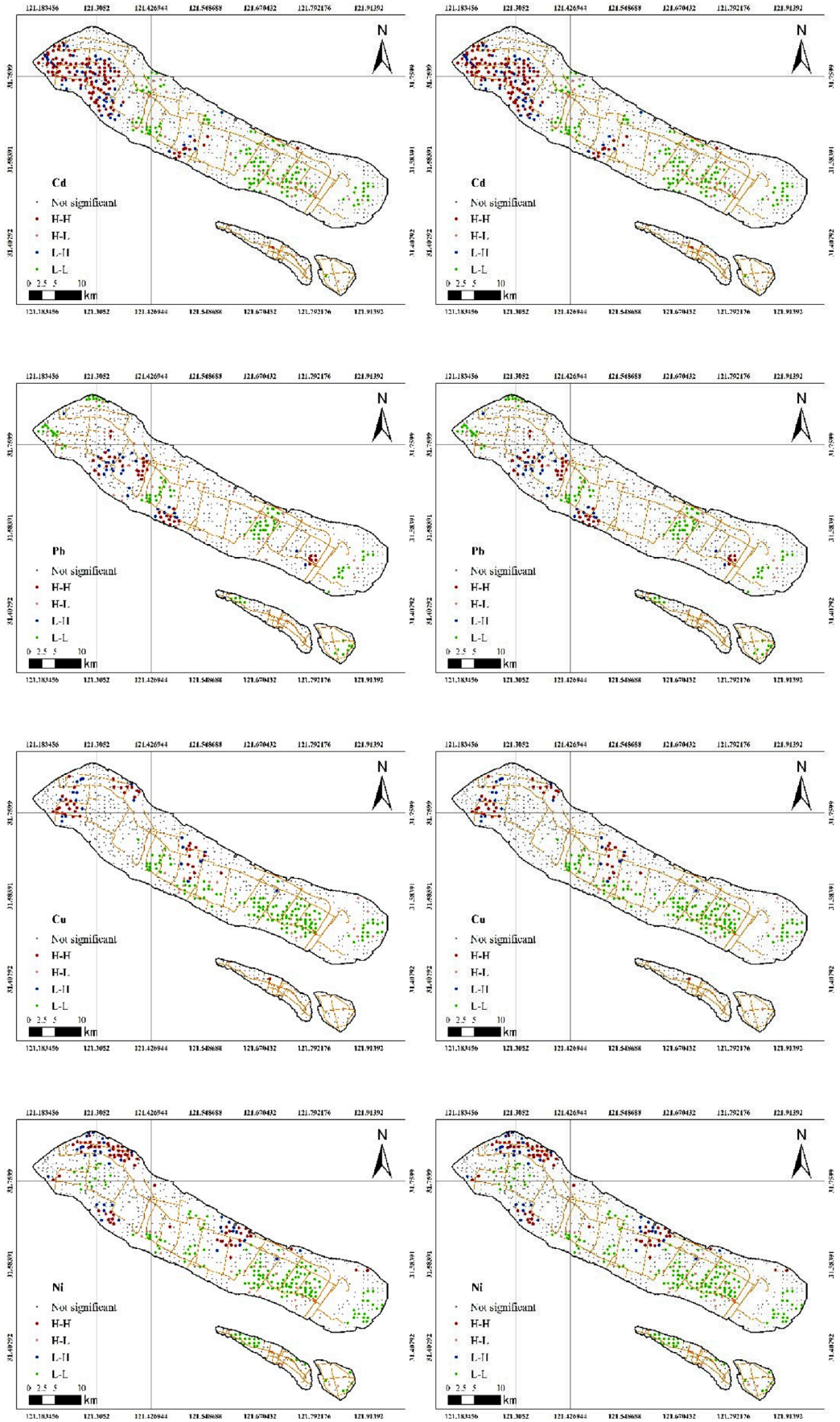

Figure 4. Local Moran's *I* cluster plots.

https://doi.org/10.1021/acsomega.4c03647
ACS Omega 2024, 9, 42734−42745

Table 3. Results of Different Exposure Paths and Noncarcinogenic Risk Assessment

element	category	HQ ing		HQ dermal		HQ inh		HI	
		adult	children	adult	children	adult	children	adult	children
As	max	4.24×10^{-02}	6.96×10^{-01}	3.66×10^{-10}	1.50×10^{-09}	4.24×10^{-04}	3.90×10^{-04}	4.28×10^{-02}	6.96×10^{-01}
	min	2.45×10^{-03}	4.02×10^{-02}	2.12×10^{-11}	8.68×10^{-11}	2.45×10^{-05}	2.25×10^{-05}	2.48×10^{-03}	4.02×10^{-02}
	average	1.87×10^{-02}	3.06×10^{-01}	1.61×10^{-10}	6.62×10^{-10}	1.87×10^{-04}	1.72×10^{-04}	1.89×10^{-02}	3.07×10^{-01}
Cd	max	2.79×10^{-04}	4.58×10^{-03}	1.21×10^{-11}	4.96×10^{-11}	1.12×10^{-04}	1.03×10^{-04}	3.91×10^{-04}	4.69×10^{-03}
	min	7.35×10^{-05}	1.21×10^{-03}	3.18×10^{-12}	1.30×10^{-11}	2.94×10^{-05}	2.70×10^{-05}	1.03×10^{-04}	1.23×10^{-03}
	average	1.37×10^{-04}	2.24×10^{-03}	5.91×10^{-12}	2.43×10^{-11}	5.47×10^{-05}	5.02×10^{-05}	1.91×10^{-04}	2.29×10^{-03}
Cr	max	3.04×10^{-02}	4.99×10^{-01}	3.94×10^{-10}	1.62×10^{-09}	1.22×10^{-02}	1.12×10^{-02}	4.25×10^{-02}	5.10×10^{-01}
	min	2.45×10^{-04}	4.02×10^{-03}	3.18×10^{-12}	1.30×10^{-11}	9.80×10^{-05}	9.01×10^{-05}	3.43×10^{-04}	4.11×10^{-03}
	average	1.55×10^{-02}	2.54×10^{-01}	2.01×10^{-10}	8.25×10^{-10}	6.20×10^{-03}	5.70×10^{-03}	2.17×10^{-02}	2.60×10^{-01}
Cu	max	2.13×10^{-03}	3.50×10^{-02}			2.13×10^{-05}	1.96×10^{-05}	2.15×10^{-03}	3.50×10^{-02}
	min	3.68×10^{-05}	6.03×10^{-04}			3.68×10^{-07}	3.38×10^{-07}	3.71×10^{-05}	6.03×10^{-04}
	average	4.71×10^{-04}	7.73×10^{-03}			4.71×10^{-06}	4.33×10^{-06}	4.76×10^{-04}	7.73×10^{-03}
Hg	max	2.43×10^{-03}	3.98×10^{-02}	1.05×10^{-12}	4.30×10^{-12}	3.47×10^{-04}	3.18×10^{-04}	2.77×10^{-03}	4.01×10^{-02}
	min	2.45×10^{-04}	4.02×10^{-03}	1.06×10^{-13}	4.34×10^{-13}	2.45×10^{-06}	3.22×10^{-05}	2.48×10^{-04}	4.05×10^{-03}
	average	1.27×10^{-03}	2.08×10^{-02}	5.48×10^{-13}	2.25×10^{-12}	1.27×10^{-05}	1.67×10^{-04}	1.28×10^{-03}	2.10×10^{-02}
Ni	max	2.24×10^{-03}	3.68×10^{-02}	2.15×10^{-10}	8.82×10^{-10}	5.61×10^{-04}	5.15×10^{-04}	2.80×10^{-03}	3.73×10^{-02}
	nin	7.35×10^{-05}	1.21×10^{-03}	7.05×10^{-12}	2.89×10^{-11}	1.84×10^{-05}	1.69×10^{-05}	9.19×10^{-05}	1.22×10^{-03}
	average	9.81×10^{-04}	1.61×10^{-02}	9.41×10^{-11}	3.86×10^{-10}	2.45×10^{-04}	2.25×10^{-04}	1.23×10^{-03}	1.63×10^{-02}
Pb	max	3.02×10^{-02}	4.96×10^{-01}	3.31×10^{-12}	1.36×10^{-11}	2.02×10^{-03}	1.86×10^{-03}	3.23×10^{-02}	4.98×10^{-01}
	min	4.20×10^{-04}	6.89×10^{-03}	4.59×10^{-14}	1.88×10^{-13}	2.81×10^{-05}	2.58×10^{-05}	4.48×10^{-04}	6.92×10^{-03}
	average	4.62×10^{-03}	7.58×10^{-02}	5.05×10^{-13}	2.07×10^{-12}	3.09×10^{-04}	2.84×10^{-04}	4.93×10^{-03}	7.61×10^{-02}
Zn	max	3.77×10^{-04}	6.19×10^{-03}			3.77×10^{-06}	3.47×10^{-06}	3.81×10^{-04}	6.20×10^{-03}
	min	2.45×10^{-06}	4.02×10^{-05}			2.45×10^{-08}	2.25×10^{-08}	2.48×10^{-06}	4.02×10^{-05}
	average	1.73×10^{-04}	2.84×10^{-03}			1.73×10^{-06}	1.59×10^{-06}	1.75×10^{-04}	2.85×10^{-03}
total risk		4.18×10^{-02}	6.86×10^{-01}	4.64×10^{-10}	1.90×10^{-09}	7.02×10^{-03}	6.60×10^{-03}	4.88×10^{-02}	6.93×10^{-01}

Table 4. Results of Different Exposure Routes and Total Carcinogenic Risk Assessment

element	category	R hand and mouth intake		R respiratory inhalation		R skin contact		RT	
		adult	children	adult	children	adult	children	adult	children
As	max	1.91×10^{-05}	3.13×10^{-04}	2.36×10^{-14}	9.67×10^{-14}	1.91×10^{-07}	1.75×10^{-07}	1.93×10^{-05}	3.13×10^{-04}
	min	1.10×10^{-06}	1.81×10^{-05}	1.36×10^{-15}	5.59×10^{-15}	1.10×10^{-08}	1.01×10^{-08}	1.11×10^{-06}	1.81×10^{-05}
	average	8.40×10^{-06}	1.38×10^{-04}	1.04×10^{-14}	4.26×10^{-14}	8.40×10^{-08}	7.72×10^{-08}	8.49×10^{-06}	1.38×10^{-04}
Cd	max			2.17×10^{-16}	8.91×10^{-16}			2.17×10^{-16}	8.91×10^{-16}
	min			5.72×10^{-17}	2.34×10^{-16}			5.72×10^{-17}	2.34×10^{-16}
	average			1.06×10^{-16}	4.36×10^{-16}			1.06×10^{-16}	4.36×10^{-16}
Cr	max	4.56×10^{-05}	7.48×10^{-04}	3.31×10^{-16}	1.36×10^{-15}	1.82×10^{-05}	1.68×10^{-05}	6.38×10^{-05}	7.65×10^{-04}
	min	3.68×10^{-07}	6.03×10^{-06}	2.67×10^{-18}	1.09×10^{-17}	1.47×10^{-07}	1.35×10^{-07}	5.15×10^{-07}	6.17×10^{-06}
	average	2.33×10^{-05}	3.81×10^{-04}	1.69×10^{-16}	6.92×10^{-16}	9.30×10^{-06}	8.55×10^{-06}	3.26×10^{-05}	3.90×10^{-04}
Ni	max			5.05×10^{-15}	2.07×10^{-14}			5.05×10^{-15}	2.07×10^{-14}
	min			1.65×10^{-16}	6.78×10^{-16}			1.65×10^{-16}	6.78×10^{-16}
	average			2.21×10^{-15}	9.05×10^{-15}			2.21×10^{-15}	9.05×10^{-15}
total risk		3.17×10^{-05}	5.19×10^{-04}	1.29×10^{-14}	5.28×10^{-14}	9.38×10^{-06}	8.62×10^{-06}	4.10×10^{-05}	5.28×10^{-04}

surrounding area. The total noncarcinogenic risk (HQ) of heavy metals in adults and children under three different exposure paths was 4.88×10^{-02} and 6.93×10^{-01}, respectively. The health risk of children was greater than that of adults but lower than the risk warning value. The carcinogenic risk R_i of the three different exposure routes is ranked from large to small as $R_{ing} > R_{dermal} > R_{inh}$. The total carcinogenic risk of different heavy metals has a descending order of Cr > As > Ni > Cd. According to the research of Hadei et al.,[66] $R > 1 \times 10^{-4}$ is defined as a clear carcinogenic risk, 1×10^{-4} to 1×10^{-5} is defined as a high probability carcinogenic risk, and 1×10^{-5} to 1×10^{-6} is defined as a possible carcinogenic risk. $R < 1 \times 10^{-6}$ is defined as a negligible carcinogenic risk, and the U.S. EPA similarly defines 1×10^{-6} as a safety threshold. The total carcinogenic risk (R_T) of multiple heavy metals for children and adults was 5.28×10^{-04} and 4.10×10^{-05}, respectively, and the carcinogenic risk was close to the risk threshold. Therefore, attention should be paid to health risks, especially to children.

4. CONCLUSIONS

The concentrations, pollution levels, spatial distributions, possible sources, and health risks of eight heavy metals in soils were explored in the Chongming District, Shanghai. The average concentrations of As, Cd, Hg, Pb, Cr, Cu, Zn, and Ni in the soil were 8.87, 0.19, 0.06, 28.75, 76.01, 37.74, 88.93, and 30.33 mg kg^{-1}, respectively. The coefficients of variation for Hg and Cu were higher than others, so some areas were seriously affected by human activities. Based on the PMF model, four origins were identified, and exact contributions

https://doi.org/10.1021/acsomega.4c03647
ACS Omega 2024, 9, 42734−42745

were calculated: 97.9% of Cr and 68.8% of Pb came from traffic sources; 87.7, 60.4, and 51.7% of Cu, Zn, and Cd, respectively, were derived from industrial sources; 100% of Hg was closely related to the exhaust gas from ship docks and bus stations; and 96.3% As and 59.3% of Ni were mainly from natural sources. Traffic sources, industrial sources, exhaust gas from ship docks and bus station sources, and natural sources were the four main contributions to heavy metals in the soils of peri-urban Shanghai Chongming Island. The validation of spatial analysis methods such as geostatistics and the Moran index showed that the analytical effect of PMF model was good, and the combined application of the receptor model and the spatial analysis method could optimize and verify the effectiveness of the analytical model and more comprehensively analyze the source of heavy metals in soil. In addition, the noncarcinogenic risks under three exposure routes are small or negligible and will not cause noncarcinogenic risks to the surrounding areas. The total noncarcinogenic risk HQ for children and adults is lower than the risk warning value, whereas the total carcinogenic risk R_T values are 5.28×10^{-04} and 4.10×10^{-05}, respectively, which are close to the risk threshold. The health risks for children deserve further attention.

■ ASSOCIATED CONTENT

Supporting Information

The Supporting Information is available free of charge at https://pubs.acs.org/doi/10.1021/acsomega.4c03647.

Population (children, adults) exposure assessment and parameters of heavy metal toxicity (Table S1); the values of RfD and SF in different exposure pathways (ingestion, dermal contact, and inhalation) of soil heavy metals (Table S2); the concentrations of eight heavy metals (As, Cd, Hg, Pb, Cr, Cu, Zn, and Ni) in the sampling site (Table S3); Kolmogorov−Smirnov test of normality (Table S4); and the concentrations of eight heavy metals after transformation in the sampling site (Table S5) (PDF)

■ AUTHOR INFORMATION

Corresponding Author

Xiurong Chen − *State Environmental Protection Key Laboratory of Environmental Risk Assessment and Control on Chemical Process, School of Resources and Environmental Engineering, East China University of Science and Technology, Shanghai 200237, China;* orcid.org/0000-0003-2544-6570; Email: xrchen@ecust.edu.cn

Authors

Cheng Shen − *State Environmental Protection Key Laboratory of Environmental Risk Assessment and Control on Chemical Process, School of Resources and Environmental Engineering, East China University of Science and Technology, Shanghai 200237, China; State Environmental Protection Engineering Center for Urban Soil Contamination Control and Remediation, Shanghai Academy of Environmental Sciences, Shanghai 200233, China;* orcid.org/0009-0002-3016-4041

Min Wang − *State Environmental Protection Engineering Center for Urban Soil Contamination Control and Remediation, Shanghai Academy of Environmental Sciences, Shanghai 200233, China*

Jinghua Su − *State Environmental Protection Engineering Center for Urban Soil Contamination Control and Remediation, Shanghai Academy of Environmental Sciences, Shanghai 200233, China*

Huilun Sun − *State Environmental Protection Key Laboratory of Environmental Risk Assessment and Control on Chemical Process, School of Resources and Environmental Engineering, East China University of Science and Technology, Shanghai 200237, China*

Wenan Hu − *School of Ecological and Environmental Sciences, East China Normal University, Shanghai 200241, China*

Kuangfei Lin − *State Environmental Protection Key Laboratory of Environmental Risk Assessment and Control on Chemical Process, School of Resources and Environmental Engineering, East China University of Science and Technology, Shanghai 200237, China*

Jian Wu − *Shanghai Technology Center for Reduction of Pollution and Carbon Emissions, Shanghai 200235, China*

Fuwen Liu − *School of Chemical and Environmental Engineering, Shanghai Institute of Technology, Shanghai 201418, China*

Chenyan Sha − *State Environmental Protection Engineering Center for Urban Soil Contamination Control and Remediation, Shanghai Academy of Environmental Sciences, Shanghai 200233, China*

Complete contact information is available at: https://pubs.acs.org/10.1021/acsomega.4c03647

Notes

The authors declare no competing financial interest.

■ ACKNOWLEDGMENTS

The authors have no conflicts of interest. All authors contributed to the study conception and design. This research was supported by the Nature Science Foundation of Shanghai Grant (19ZR1444100 and 21DZ1201700) and Shanghai Sailing Program (23YF1445900). All authors commented on previous versions of the manuscript. All authors read and approved the final manuscript. We also would like to thank the anonymous referees for their valuable comments.

■ REFERENCES

(1) Lv, J.; Liu, Y. An integrated approach to identify quantitative sources and hazardous areas of heavy metals in soils. *Sci. Total Environ.* **2019**, *646*, 19−28.

(2) Fei, X.; Lou, Z.; Xiao, R.; Ren, Z.; Lv, X. Contamination assessment and source apportionment of heavy metals in agricultural soil through the synthesis of PMF and GeogDetector models. *Sci. Total Environ.* **2020**, *747*, No. 141293.

(3) Tepanosyan, G.; Sahakyan, L.; Belyaeva, O.; Maghakyan, N.; Saghatelyan, A. Human health risk assessment and riskiest heavy metal origin identification in urban soils of Yerevan, Armenia. *Chemosphere* **2017**, *184*, 1230−1240.

(4) Zhao, K.; Fu, W.; Qiu, Q.; Ye, Z.; Li, Y.; Tunney, H.; Dou, C.; Zhou, K.; Qian, X. Spatial patterns of potentially hazardous metals in paddy soils in a typical electrical waste dismantling area and their pollution characteristics. *Geoderma* **2019**, *337*, 453−462.

(5) Gemeda, F. T.; Guta, D. D.; Wakjira, F. S.; Gebresenbet, G. Occurrence of heavy metal in water, soil, and plants in fields irrigated with industrial wastewater in Sabata town. *Ethiopia. Environmental Science and Pollution Research* **2021**, *28*, 12382−12396.

(6) Aelion, C. M.; Davis, H. T.; McDermott, S.; Lawson, A. B. Soil metal concentrations and toxicity: Associations with distances to

industrial facilities and implications for human health. *Sci. Total Environ.* **2009**, *407*, 2216−2223.
(7) Long, Z.; Zhu, H.; Bing, H.; Tian, X.; Wang, Z.; Wang, X.; Wu, Y. Contamination, sources and health risk of heavy metals in soil and dust from different functional areas in an industrial city of Panzhihua City, Southwest China. *Journal of Hazardous Materials* **2021**, *420*, No. 126638.
(8) Ju, Y.; Luo, Z.; Bi, J.; Liu, C.; Liu, X. Transfer of heavy metals from soil to tea and the potential human health risk in a regional high geochemical background area in southwest China. *Science of The Total Environment* **2024**, *908*, No. 168122.
(9) Duruibe, J. O.; Ogwoegbu, M. O. C.; Egwurugwu, J. N. Heavy Metal Pollution and Human Biotoxic Effects. *Int. J. Phys. Sci.* **2007**, *2*, 112−118.
(10) Gowd, S. S.; Reddy, M. R.; Govil, P. K. Assessment of heavy metal contamination in soils at Jajmau (Kanpur) and Unnao industrial areas of the Ganga Plain, Uttar Pradesh, India. *J. Hazard. Mater.* **2010**, *174*, 113−121.
(11) Mielke, H. W.; Gonzales, C. R.; Smith, M. K.; Mielke, P. W. The Urban Environment and Children's Health: Soils as an Integrator of Lead, Zinc, and Cadmium in New Orleans, Louisiana, U.S.A. *Environmental Research* **1999**, *81*, 117−129.
(12) Shifaw, E. Review of Heavy Metals Pollution in China in Agricultural and Urban Soils. *Journal of Health Pollution* **2018**, *8*, No. 180607.
(13) Abrahams, P. W. Soils: their implications to human health. *Sci. Total Environ.* **2002**, *291*, 1−32.
(14) Briffa, J.; Sinagra, E.; Blundell, R. Heavy metal pollution in the environment and their toxicological effects on humans. *Heliyon* **2020**, *6*, e04691−e04691.
(15) Olawoyin, R.; Oyewole, S. A.; Grayson, R. L. Potential risk effect from elevated levels of soil heavy metals on human health in the Niger delta. *Ecotoxicology and Environmental Safety* **2012**, *85*, 120−130.
(16) Dong, B.; Zhang, R.; Gan, Y.; Cai, L.; Freidenreich, A.; Wang, K.; Guo, T.; Wang, H. Multiple methods for the identification of heavy metal sources in cropland soils from a resource-based region. *Sci. Total Environ.* **2019**, *651*, 3127−3138.
(17) Chrastný, V.; Šillerová, H.; Vítková, M.; Francová, A.; Jehlička, J.; Kocourková, J.; Aspholm, P. E.; Nilsson, L. O.; Berglen, T. F.; Jensen, H. K. B.; Komárek, M. Unleaded gasoline as a significant source of Pb emissions in the Subarctic. *Chemosphere* **2018**, *193*, 230−236.
(18) Liu, S.; Yan, X.; Shi, B.; Liu, Z.; Yan, X.; Wang, X.; Zhou, Y.; Liang, T. Utilizing machine learning algorithm for finely three-dimensional delineation of soil-groundwater contamination in a typical industrial park, North China: importance of multisource auxiliary data. *Sci. Total Environ.* **2024**, *911*, No. 168598.
(19) Zhang, Q.; Han, G.; Liu, M.; Liang, T. Spatial distribution and controlling factors of heavy metals in soils from Puding Karst Critical Zone Observatory, southwest China. *Environ. Earth Sci.* **2019**, *78*, 279.
(20) Yang, X.; You, M.; Liu, S.; Sarkar, B.; Liu, Z.; Yan, X. Microbial responses towards biochar application in potentially toxic element (PTE)contaminated soil: a critical review on effects and potential mechanisms. *Biochar* **2023**, *5*, 57.
(21) Chen, T.; Zheng, Y.; Lei, M.; Huang, Z.; Wu, H.; Chen, H.; Fan, K.; Yu, K.; Wu, X.; Tian, Q. Assessment of heavy metal pollution in surface soils of urban parks in Beijing, China. *Chemosphere* **2005**, *60*, 542−551.
(22) Islam, S.; Ahmed, K.; Habibullah-Al-Mamun; Masunaga, S. Potential ecological risk of hazardous elements in different land-use urban soils of Bangladesh. *Sci. Total Environ.* **2015**, *512*−*513*, 94−102.
(23) Maanan, M.; Saddik, M.; Maanan, M.; Chaibi, M.; Assobhei, O.; Zourarah, B. Environmental and ecological risk assessment of heavy metals in sediments of Nador lagoon, Morocco. *Ecological Indicators* **2015**, *48*, 616−626.
(24) Meng, X. F.; Guo, J. M.; Yang, J. X.; Yang, J.; Zheng, G. D.; Qiao, P. W.; Bian, J. L.; Chen, T. B. Spatial distribution and risk assessment of heavy metal pollution in farmland soils surrounding a typical industrial area of Henan province. *Chin. J. Environ. Sci.* **2021**, *42*, 900−908.
(25) Abuduwailil, J.; Zhaoyong, Z.; Fengqing, J. Evaluation of the pollution and human health risks posed by heavy metals in the atmospheric dust in Ebinur Basin in Northwest China. *Environ. Sci. Pollut. Res.* **2015**, *22*, 14018−14031.
(26) Amjadian, K.; Pirouei, M.; Mehr, M. R.; Shakeri, A.; Rasool, S. K.; Haji, D. I. Contamination, health risk, mineralogical and morphological status of street dusts- case study: Erbil metropolis, Kurdistan Region-Iraq. *Environ. Pollut.* **2018**, *243*, 1568−1578.
(27) Zou, M.; Zhou, S.; Zhou, Y.; Jia, Z.; Guo, T.; Wang, J. Cadmium pollution of soil-rice ecosystems in rice cultivation dominated regions in China: A review. *Environ. Pollut.* **2021**, *280*, No. 116965.
(28) Manousakas, M.; Furger, M.; Daellenbach, K. R.; Canonaco, F.; Chen, G.; Tobler, A.; Rai, P.; Qi, L.; Tremper, A. H.; Green, D.; Hueglin, C.; Slowik, J. G.; Haddad, I. E.; Prevot, A. S. H. Source identification of the elemental fraction of particulate matter using size segregated, highly time-resolved data and an optimized source apportionment approach. *Atmos. Environ.: X* **2022**, *14*, No. 100165.
(29) Sakizadeh, M.; Zhang, C. Source identification and contribution of land uses to the observed values of heavy metals in soil samples of the border between the Northern Ireland and Republic of Ireland by receptor models and redundancy analysis. *Geoderma* **2021**, *404*, No. 115313.
(30) PriyaDarshini, S.; Sharma, M.; Singh, D. Synergy of receptor and dispersion modelling: Quantification of PM_{10} emissions from road and soil dust not included in the inventory. *Atmospheric Pollution Research* **2016**, *7*, 403−411.
(31) Luo, H.; Wang, Q.; Guan, Q.; Ma, Y.; Ni, F.; Yang, E.; Zhang, J. Heavy metal pollution levels, source apportionment and risk assessment in dust storms in key cities in Northwest China. *Journal of Hazardous Materials* **2022**, *422*, No. 126878.
(32) Paatero, P.; Tapper, U. Positive matrix factorization: A non-negative factor model with optimal utilization of error estimates of data values. *Environmetrics* **1994**, *5*, 111−126.
(33) Anaman, R.; Peng, C.; Jiang, Z.; Liu, X.; Zhou, Z.; Guo, Z.; Xiao, X. Identifying sources and transport routes of heavy metals in soil with different land uses around a smelting site by GIS based PCA and PMF. *Sci. Total Environ.* **2022**, *823*, No. 153759.
(34) Mokhtarzadeh, Z.; Keshavarzi, B.; Moore, F.; Marsan, F. A.; Padoan, E. Potentially toxic elements in the Middle East oldest oil refinery zone soils: source apportionment, speciation, bioaccessibility and human health risk assessment. *Environmental Science and Pollution Research* **2020**, *27*, 40573−40591.
(35) Guan, X. X.; Zhou, X. P.; Lei, C. N.; Peng, Y. W.; Zhang, S. L. Source apportionment of soils PAHs in Lanzhou based on GIS and APCS-MLR model. *Chin. J. Environ. Sci.* **2021**, *42*, 3904−3912.
(36) Gulgundi, M. S.; Shetty, A. Source Apportionment of Groundwater Pollution using Unmix and Positive Matrix Factorization. *Environmental Processes* **2019**, *6*, 457−473.
(37) Liao, S.; Jin, G.; Khan, M. A.; Zhu, Y.; Duan, L.; Luo, W.; Jia, J.; Zhong, B.; Ma, J.; Ye, Z.; Liu, D. The quantitative source apportionment of heavy metals in peri-urban agricultural soils with UNMIX and input fluxes analysis. *Environ. Technol. Innovation* **2020**, *21*, No. 101232.
(38) Loredo, J.; Ordóñez, A.; Charlesworth, S.; De Miguel, E. Influence of industry on the geochemical urban environment of Mieres (Spain) and associated health risk. *Environ. Geochem. Health* **2003**, *25*, 307−323.
(39) Liu, Z.; Wang, L.; Yan, M.; Ma, B.; Cao, R. Source apportionment of soil heavy metals based on multivariate statistical analysis and the PMF model: A case study of the Nanyang Basin, China. *Environ. Technol. Innovation* **2024**, *33*, No. 103537.
(40) Shi, B.; Yang, X.; Liang, T.; Liu, S.; Yan, X.; Li, J.; Liu, Z. Source apportionment of soil PTE in a northern industrial county using PMF model: Partitioning strategies and uncertainty analysis. *Environmental Research* **2024**, *252*, No. 118855.

https://doi.org/10.1021/acsomega.4c03647
ACS Omega 2024, 9, 42734−42745

(41) Maas, S.; Scheifler, R.; Benslama, M.; Crini, N.; Lucot, E.; Brahmia, Z.; Benyacoub, S.; Giraudoux, P. Spatial distribution of heavy metal concentrations in urban, suburban and agricultural soils in a Mediterranean city of Algeria. *Environ. Pollut.* **2010**, *158*, 2294−2301.
(42) Boudia, H.; Vassalo, L.; Hadjel, M.; Prudent, P.; Boudenne, J. L. Spatial contamination and health risks of heavy metal(loid) s in surface soils from a petrochemical complex in the north-eastern region of Algeria. *International Journal of Environmental Science and Technology* **2019**, *16*, 4707−4718.
(43) Liu, Z. Y.; Fei, Y.; Shi, H. D.; Mo, L.; Qi, J. X.; Wang, C. Source apportionment of soil heavy metals in Rucheng Country of Hunan province based on UNMIX model combined with Moran index. *Res. Environ. Sci.* **2021**, *34*, 2446−2458.
(44) Han, L.; Xu, X. B. Quantitative evaluation of human health risk of heavy metals in soils based on positive matrix factorization model and geo-statistics. *Chin. J. Environ. Sci.* **2020**, *41*, 5114−5124.
(45) Guan, Q.; Wang, F.; Xu, C.; Pan, N.; Lin, J.; Zhao, R.; Yang, Y.; Luo, H. Source apportionment of heavy metals in agricultural soil based on PMF: a case study in Hexi corridor, Northwest China. *Chemosphere* **2018**, *193*, 189−197.
(46) Chen, H.; Teng, Y.; Li, J.; Wu, J.; Wang, J. Source apportionment of trace metals in river sediments: A comparison of three methods. *Environ. Pollut.* **2016**, *211*, 28−37.
(47) Zhang, Y.; Wu, Y.; Song, B.; Zhou, L.; Wang, F.; Pang, R. Spatial distribution and main controlling factor of cadmium accumulation in agricultural soils in Guizhou. *China. Journal of Hazardous Materials* **2022**, *424*, No. 127308.
(48) USEPA *Supplemental Guidance for Developing Soil Screening Levels for Superfund Sites*; Office of Solid Waste and Remedial Response: Washington, DC, 2001.
(49) Cui, Y.; Bai, L.; Li, C.; He, Z.; Liu, X. Assessment of heavy metal contamination levels and health risks in environmental media in the northeast region. *Sustainable Cities and Society* **2022**, *80*, No. 103796.
(50) Hakanson, L. An Ecological Risk Index for Aquatic Pollution Control-A Sedimentological Approach. *Water Res.* **1980**, *14*, 975−1001.
(51) Yan, G.; Mao, L.; Jiang, B.; Chen, X.; Gao, Y.; Chen, C.; Li, F.; Chen, L. The source apportionment, pollution characteristic and mobility of Sb in roadside soils affected by traffic and industrial activities. *Journal of Hazardous Materials* **2020**, *384*, No. 121352.
(52) Cai, L.; Wang, Q.; Wen, H.; Luo, J.; Wang, S. Heavy metals in agricultural soils from a typical township in Guangdong Province, China: Occurrences and spatial distribution. *Ecotoxicology and Environmental Safety* **2019**, *168*, 184−191.
(53) Ayoubi, S.; Adman, V.; Yousefifard, M. Use of magnetic susceptibility to assess metals concentration in soils developed on a range of parent materials. *Ecotoxicology and Environmental Safety* **2019**, *168*, 138−145.
(54) Proshad, R.; Islam, M. S.; Kormoker, T.; Sayeed, A.; Khadka, S.; Idris, A. M. Potential toxic metals (PTMs) contamination in agricultural soils and foodstuffs with associated source identification and model uncertainty. *Sci. Total Environ.* **2021**, *789*, No. 147962.
(55) Kumar, S.; Rahman, M. A.; Islam, M. R.; Hashem, M. A.; Rahman, M. M. Lead and other elements-based pollution in soil, crops and water near a lead-acid battery recycling factory in Bangladesh. *Chemosphere* **2022**, *290*, No. 133288.
(56) Xie, X. J.; Kang, J. C.; Li, W. J.; Wang, G. D.; Yan, G. D.; Zhang, J. P. Analysis on heavy metal concentrations in agricultural soils of Baoshan, Shanghai. *Chin. J. Environ. Sci.* **2010**, *31*, 768−774.
(57) Negahban, S.; Mokarram, M. Potential Ecological Risk Assessment of Ni, Cu, Zn, Cd, and Pb in Roadside Soils. *Earth Space Sci.* **2021**, *8*, No. e2020EA001120.
(58) Huang, C.; Hu, Q.; Wang, H.; Qiao, L.; Jing, S.; Wang, H.; Zhou, M.; Zhu, S.; Ma, Y.; Lou, S.; Li, L.; Tao, S.; Li, Y.; Lou, D. Emission factors of particulate and gaseous compounds from a large cargo vessel operated under real-world conditions. *Environ. Pollut.* **2018**, *242*, 667−674.
(59) Doabi, S. A.; Karami, M.; Afyuni, M.; Yeganeh, M. Pollution and health risk assessment of heavy metals in agricultural soil, atmospheric dust and major food crops in Kermanshah province, Iran. *Ecotoxicology and Environmental Safety* **2018**, *163*, 153−164.
(60) Hayyat, M. S.; Adnan, M.; Khan, M. A. B.; Abd-Ur-Rahman, H.; Ahmed, R.; Fazal-ur-Rehman; Toor, M. D.; Bilal, H. M. Effect of heavy metal (Ni) on plants and soil: A review. *Int. J. Appl. Res.* **2020**, *6*, 313−318.
(61) Zhou, Y. L.; Yang, Z. B.; Wang, Q. L.; Wang, C. W.; Liu, F.; Song, Y. T.; Guo, Z. J. Potential ecological risk assessment and source analysis of heavy metals in soil-crop system in Xiong'an new district. *Chin. J. Environ. Sci.* **2021**, *42*, 2003−2015.
(62) Hu, M. J.; Li, C. Y.; Li, N. N.; Ji, T. Q.; Zheng, D. Y. Using the Matter-Element Extension Model to Assess Heavy Metal Pollution in Topsoil in Parks in the Main District Park of Lanzhou City. *Chin. J. Environ. Sci.* **2021**, *42*, 2457−2468.
(63) Huang, H.; Zhou, Y.; Liu, Y. J.; Xiao, L.; Li, K.; Duan, J. S.; Wei, H. L. Source analysis of heavy metals in farmland based on environmental variables and random forest approach: district of Xiangzhou district in Xiangyang City. *Acta Sci. Circumstantiae* **2020**, *40*, 4548−4558.
(64) Wang, J.; Wu, H.; Wei, W.; Xu, C.; Tan, X.; Wen, Y.; Lin, A. Health risk assessment of heavy metal(loid)s in the farmland of megalopolis in China by using APCS-MLR and PMF receptor models: Taking Huairou District of Beijing as an example. *Sci. Total Environ.* **2022**, *835*, No. 155313.
(65) Wang, S.; Kalkhajeh, Y.; Qin, Z.; Jiao, W. Spatial distribution and assessment of the human health risks of heavy metals in a retired petrochemical industrial area, south China. *Environmental Research* **2020**, *188*, No. 109661.
(66) Hadei, M.; Shahsavani, A.; Hopke, P. K.; Naseri, S.; Yazdanbakhsh, A.; Sadani, M.; Mesdaghinia, A.; Yarahmadi, M.; Rahmatinia, M.; Fallah, S.; Emam, B.; Kermani, M.; Jaafarzadeh, N.; Alipour, M.; Hassanzadeh, V.; Bazzazpour, S.; Nazari, S. S. H. A systematic review and meta-analysis of human biomonitoring studies on exposure to environmental pollutants in Iran. *Ecotoxicology and Environmental Safety* **2021**, *212*, No. 111986.

https://doi.org/10.1021/acsomega.4c03647
ACS Omega 2024, 9, 42734−42745